

Review

Enhancement of Brillouin Scattering Signal in Perfluorinated Graded-Index Polymer Optical Fibers

Yosuke Mizuno * and Kentaro Nakamura

Precision and Intelligence Laboratory, Tokyo Institute of Technology, 4259 Nagatsuta, Midori-ku, Yokohama 226-8503, Japan; E-Mail: knakamur@sonic.pi.titech.ac.jp

* Author to whom correspondence should be addressed; E-Mail: ymizuno@sonic.pi.titech.ac.jp; Tel.: +81-45-924-5052; Fax: +81-45-924-5091.

Received: 26 December 2011; in revised form: 18 January 2012 / Accepted: 20 January 2012 / Published: 31 January 2012

Abstract: Perfluorinated graded-index polymer optical fibers (PFGI-POFs), fabricated by replacing the hydrogen atoms of standard polymethyl methacrylate-based POFs with fluorine atoms, have been extensively studied due to their relatively low propagation loss even at telecommunication wavelength. Recently, Brillouin scattering, which is one of the most significant nonlinear effects in optical fibers, has been successfully observed in PFGI-POFs at 1.55- μm wavelength. The Brillouin Stokes signal was, however, not large enough for practical applications or for detailed investigations of the Brillouin properties. In this paper, we review our recent work on Stokes signal enhancement. First, we induce stimulated Brillouin scattering based on the so-called pump-probe technique, and discuss its applicability to temperature sensors. Then, we investigate the influence of the core diameter and length of PFGI-POFs on Stokes signal, and observe the Brillouin linewidth narrowing effect. We believe our work is an important technological step toward the implementation of practical Brillouin-based devices and systems including distributed strain and temperature sensors.

Keywords: Brillouin scattering; Brillouin gain spectrum; perfluorinated graded-index polymer optical fiber; pump-probe technique; fiber-optic sensing; distributed temperature sensing; nonlinear optics

1. Introduction

Polymer optical fibers (POFs) [1,2] have attracted considerable attention for the past several decades due to their extremely easy and cost-effective connection, high safety, and high flexibility [3] compared to conventional glass fibers. Therefore, in spite of their propagation loss being higher than that of silica glass fibers, POFs have been made use of in medium-range communication applications such as home networks and automobiles [4] as well as in high-strain monitoring applications [3,5].

On the other hand, Brillouin scattering in optical fibers [6,7], one of the most significant nonlinear processes, has been extensively studied, and a great number of useful applications have been reported so far, such as optical amplification [7], lasing [7,8], optical comb generation [8], microwave signal processing [9], slow light generation [10], phase conjugation [11], tunable delay [12], optical storage [13], core alignment of butt-coupling [14], and strain/temperature sensing [15–18]. For the purpose of improving the performance of these applications, Brillouin scattering has been investigated not only in silica single-mode fibers (SMFs) but also in some specialty fibers. They include, for example, silica multimode fibers (MMFs) [14], tellurite glass fibers [19,20], chalcogenide glass fibers [21,22], bismuth-oxide glass fibers [23,24], and photonic crystal fibers (PCFs) [25,26].

Recently, we have succeeded in observing spontaneous Brillouin scattering (SpBS) in POFs, for the first time to the best of our knowledge, at the telecommunication wavelength of 1.55 μm [27,28], which will offer many advantages of POFs to the conventional Brillouin application fields. The POFs used in the experiment were cyclic transparent optical polymer (CYTOP)-based perfluorinated graded-index (PFGI-) POFs, which are fabricated by replacing the hydrogen atoms of standard polymethyl methacrylate (PMMA)-based POFs with fluorine atoms. Their detailed structure and fabrication method are well summarized in [29]. Their Brillouin gain coefficient was estimated to be approximately 3.09×10^{-11} m/W, which was almost the same as that of silica SMFs, indicating that Brillouin scattering in PFGI-POFs can be applied to a variety of practical devices and systems in the same way as Brillouin scattering in silica SMFs. We have also investigated the dependences of the Brillouin frequency shift (BFS) on strain and temperature in a PFGI-POF at 1.55 μm , and found that SpBS in PFGI-POFs can be potentially utilized to develop high-accuracy temperature sensors with reduced strain sensitivity [30]. Small Brillouin Stokes signal was, however, a major problem to be solved for practical future applications as well as for detailed investigations of the Brillouin gain spectrum (BGS).

In this review, we summarize two methods to enhance the Brillouin Stokes signal. First, stimulated Brillouin scattering (SBS) is induced using the so-called pump-probe technique [31], and its applicability to temperature sensors is discussed. Second, the influence of the core diameter and length of the PFGI-POFs is investigated [32], which will be a good guideline for designing PFGI-POF structures suitable for future applications.

2. Brillouin Scattering in Optical Fibers

When a light beam is injected into a fiber under test (FUT), it interacts with acoustic phonons, generating backscattered light called Stokes light. This phenomenon is called SpBS. Since the phonons decay exponentially, the backscattered Brillouin light spectrum, known as BGS, takes the shape of

Lorentzian function with the bandwidth of several tens of MHz. If the power of the pump light is higher than the Brillouin threshold power P_{th} , the Stokes light caused by SpBS acts as a seed of stimulated scattering, and there occurs a transition from SpBS to SBS. As a result, the power of the Stokes light is drastically enhanced. P_{th} is given as [7]

$$P_{th} = \frac{21 b A_{eff}}{K g_B L_{eff}} \quad (1)$$

where b is the correction factor for multimode fibers [33], which can be treated as 2 when the numerical aperture (NA) is ~ 0.2 ; A_{eff} is the effective cross-sectional area, which is approximately in proportion to the core diameter for multimode fibers [34,35]; K is the polarization coefficient, which is 1, if polarization is maintained and 0.667 otherwise; g_B is the Brillouin gain coefficient; and L_{eff} is the effective fiber length defined as

$$L_{eff} = [1 - \exp(-\alpha L)] / \alpha \quad (2)$$

where α is the propagation loss and L is the fiber length.

Both in SpBS and in SBS, the frequency where the peak power is obtained in the BGS is downshifted by several GHz from the incident light frequency, and the amount of this frequency shift is called BFS. In optical fibers, the BFS ν_B is given by [7]

$$\nu_B = \frac{2n v_A}{\lambda_p} \quad (3)$$

where n is the refractive index, v_A is the acoustic velocity in the fiber, λ_p is the wavelength of the incident pump light. If tensile strain is applied or temperature is changed in a standard silica SMF, the BFS moves to higher frequency in proportion to the applied strain (+580 MHz/%) [36] and the temperature change (+1.18 MHz/K) [37]. In some specialty fibers, such as tellurite glass fibers, it is known that the BFS moves to lower frequency with increasing applied strain (−230 MHz/%) [20] and temperature (−1.14 MHz/K) [24]. In both cases, we can derive the strain amplitude and temperature change by measuring the BFS in the fiber.

3. Spontaneous Brillouin Scattering in PFGI-POFs

A standard POF composed of PMMA [1,2] is optimally designed for light transmission at 650 nm, with propagation loss of ~ 200 dB/km. Its loss at telecommunication wavelength is, however, so high ($\gg 1 \times 10^5$ dB/km) that the Brillouin signal cannot be detected. In the meantime, in order to observe Brillouin scattering in a PMMA-based POF at 650 nm, we are required to prepare all the necessary optical devices at this wavelength, which are not easy from the viewpoint of availability and cost. Therefore, instead of PMMA-based POFs, we used PFGI-POFs with lower loss (~ 250 dB/km) even at 1.55 μm , which is the optimal wavelength for long distance data transmission in silica optical fibers.

Up to now, the spontaneous Brillouin scattering properties in a PFGI-POF with 120- μm core diameter have been investigated at 1.55 μm [27]. The BFS and the Brillouin linewidth were 2.83 GHz and 105 MHz, respectively. Using these values, the Brillouin gain coefficient was calculated to be 3.09×10^{-11} m/W, which is almost the same as that of standard silica SMFs and higher than that of silica

GI-MMFs. Here, we should bear in mind that the actual Brillouin gain coefficient may be higher than this value due to the multimode nature of the PFGI-POF. The Brillouin threshold power of a 100-m PFGI-POF was estimated to be as high as 24 W, and the Stokes signal was not sufficiently large to be applied to practical devices and systems.

The BFS dependences on strain and temperature in a 5-m PFGI-POF have also been investigated at 1.55 μm [30]. They showed negative dependences with coefficients of -121.8 MHz/% and -4.09 MHz/K, respectively, which are -0.2 and -3.5 times as large as those in silica fibers. These BFS dependences were found to originate from the dependences of the Young's modulus on strain and temperature. Thus, Brillouin scattering in PFGI-POFs has a big potential for high-accuracy temperature sensing with reduced strain sensitivity.

4. Enhancement of Brillouin Stokes Signal (I): Induction of Stimulated Scattering

In this Section, we describe the observation of SBS in a PFGI-POF with 120- μm core diameter at 1.55 μm with pump-probe technique [31]. The BGS is detected with extremely high S/N ratio, even with a 1-m PFGI-POF, scrambled polarization state, and no averaging. We also investigate the BGS dependences on probe power and temperature, and confirm that SBS in a PFGI-POF measured with this technique can be utilized to develop high-accuracy temperature sensors as well.

4.1. Motivation and Principle

The Brillouin scattering in PFGI-POFs observed in the previous experimental setup [27,28] was not stimulated but spontaneous, because the Brillouin threshold of PFGI-POFs was estimated to be as high as 24 W, as already described in Section 3. Consequently, the power of the reflected Stokes light was so low that we had to face the following four problems: (1) a PFGI-POF longer than several meters was required, (2) the polarization state had to be optimized, (3) averaging of the spectral data had to be conducted several tens of times, and (4) signal-to-noise (S/N) ratio of the BGS was quite low, even when (1), (2), and (3) were cleared. In order to implement practical Brillouin sensors and other systems using PFGI-POFs, these problems need to be resolved.

One solution is to employ so-called pump-probe technique. As described in Section 2, when the pump power is higher than the Brillouin threshold, a transition from SpBS to SBS occurs, leading to drastic enhancement of the Stokes light. On the other hand, when probe light at the same frequency as the Stokes light is also injected into the other end of the FUT, SBS is induced even when the power of the pump light is much lower than the Brillouin threshold, because the probe light itself acts as a seed of stimulated scattering [38]. This technique, called pump-probe technique, has been used to develop Brillouin systems with high S/N ratio [17].

4.2. Experimental Setup

The FUT used in the experiment was a 1-m PFGI-POF (Asahi Glass Co., Ltd., 2009) with a core diameter of 120 μm , NA of 0.185, a core refractive index of ~ 1.35 , and propagation loss of ~ 250 dB/km at 1.55 μm (manufacturer's specifications). The experimental setup is schematically shown in Figure 1, which is similar to that of Brillouin optical correlation-domain analysis (BOCDA) [16,17].

The light beam from a 1550-nm three-electrode laser diode (LD) was divided into two. One was used as the pump light, after being chopped with an intensity modulator (IM) for lock-in detection and being amplified with an erbium-doped fiber amplifier (EDFA). The other was used as the probe light, after passing two EDFAs, a single-sideband modulator (SSBM), and a polarization scrambler (PSCR). The SSBM was employed with a microwave generator (MG) and a proper DC bias control to suppress the carrier (pump) and the anti-Stokes component of the two first-order sidebands and to maintain a stable frequency downshift from the pump light. This frequency downshift was swept from 2.5 GHz to 3.5 GHz with a period of 300 ms to obtain the BGS of the PFGI-POF, which is observed approximately at 2.8 GHz. The suppression ratio of the other frequency components was kept higher than 25 dB, as shown in Figure 2.

Figure 1. Experimental setup for observing stimulated Brillouin scattering (SBS) in perfluorinated graded-index polymer optical fibers (PFGI-POFs) with pump-probe technique: LD, laser diode; EDFA, erbium-doped fiber amplifier; FG, function generator; FUT, fiber under test; IM, intensity modulator; ISO, isolator; LI-A, lock-in amplifier; MG, microwave generator; OSC, oscilloscope; PD, photo-detector; POF, polymer optical fiber; PSCR: polarization scrambler; SSBM, single-sideband modulator; VOA, variable optical attenuator.

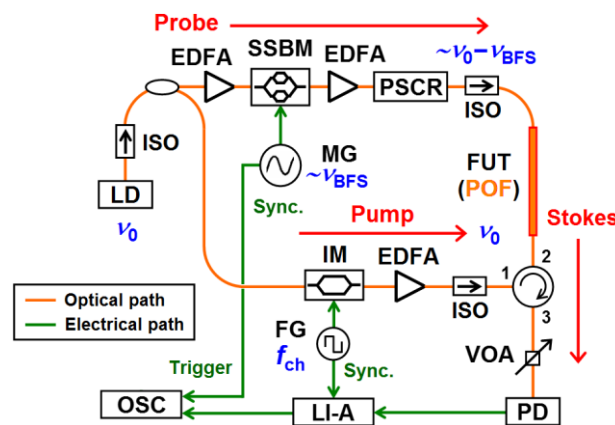
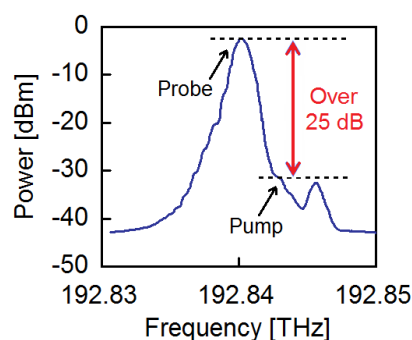


Figure 2. Measured optical spectrum of the SSBM output when the frequency of the MG was set to 2.83 GHz.



The PSCR, which can modulate the polarization state at 1 MHz, was inserted to suppress the polarization-dependent fluctuations of the signal. The PFGI-POF and the silica SMFs were butt-coupled [27] with the gaps filled with index matching oil ($n = 1.46$) to minimize the Fresnel reflection. The Stokes

light was adjusted in power with a variable optical attenuator (VOA), and converted to an electrical signal with a 125-MHz photo-detector (PD). After passing a lock-in amplifier (LI-A) with a chopping frequency of 5.018 MHz and a time constant of 10 ms, the electrical signal was observed as a BGS with an oscilloscope (OSC) synchronized with the frequency sweep of the SSBM.

4.3. Experimental Results

Figure 3 shows the measured BGS without averaging when the pump power and the probe power were 23 dBm and 22 dBm, respectively. The power was normalized so that the peak power was 1.0. Although the PFGI-POF length was only 1 m and the polarization state was scrambled, the BGS was observed with much higher S/N ratio than that previously reported [30]. The BFS was 2.86 GHz, which is slightly higher than the previously reported value of 2.83 GHz [27]. This discrepancy seems to originate from the difference in temperature and the time constant of the LI-A which is not short enough. The 3-dB bandwidth of the BGS measured in this experiment was about 160 MHz, but further research is needed on the bandwidth because it is also dependent on the time constant of the LI-A (Note that, when the time constant was shorter than 10 ms, the BGS was distorted).

Figure 3. BGS in PFGI-POF observed without averaging.

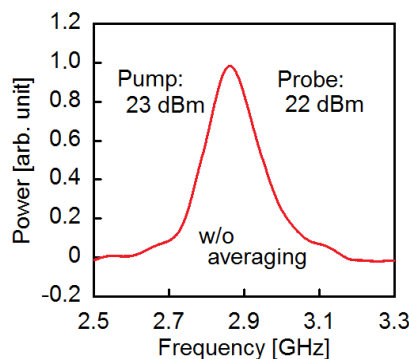
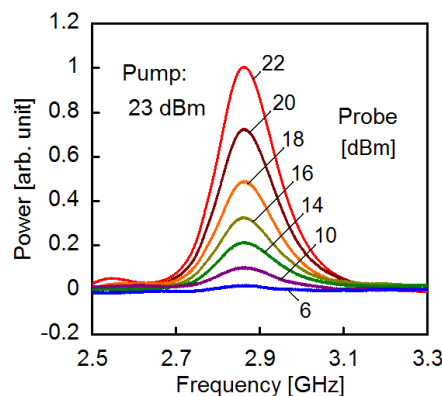


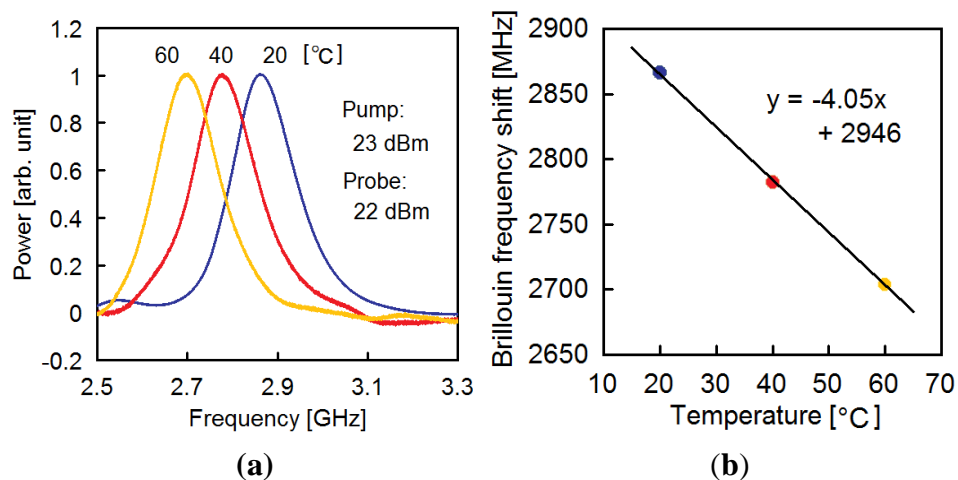
Figure 4 shows the dependence of the BGS on probe power when the pump power was fixed at 23 dBm. The probe power was reduced from 22 dBm down to 6 dBm, and averaging was conducted 30 times for the observable readout when the Stokes power was very low. As the probe power decreased, the Stokes power also decreased, which proves that this BGS is caused by the interaction between the pump light and the probe light, *i.e.*, SBS.

Figure 4. Dependence of BGS on probe power in PFGI-POF.



The dependence of the BGS on temperature was also measured as shown in Figure 5(a). The pump power and the probe power were 23 dBm and 22 dBm, respectively, and averaging was conducted 30 times. The temperature was set to 20, 40, and 60 °C. With the increasing temperature, the BGS shifted toward lower frequency. The temperature dependence of the BFS is shown in Figure 5(b). The slope of -4.05 MHz/K is in good agreement with the previous report [30], which confirms that the BGS in a PFGI-POF observed with the pump-probe technique can be applied to high-accuracy temperature sensing.

Figure 5. Dependence of (a) BGS and (b) BFS on temperature in PFGI-POF.



4.4. Summary

The SBS in a PFGI-POF was successfully observed at 1.55 μm with pump-probe technique. We detected the BGS with extremely high S/N ratio, even with a 1-m PFGI-POF, scrambled polarization state, and no averaging. We also investigated the BGS dependence on probe power, which proved that the measured BGS was caused not by SpBS but by SBS. Besides, we measured the BGS dependence on temperature, showing that BGS in a PFGI-POF observed with this technique can be applied to temperature sensing with high accuracy. We are sure that use of SBS with large Stokes signal will be indispensable in developing Brillouin-based distributed temperature/strain sensing systems using PFGI-POFs.

5. Enhancement of Brillouin Stokes Signal (II): Influence of Core Diameter and Fiber Length

In this Section, we describe the characterization on the BGS in PFGI-POFs with 62.5- μm core diameter [32]. First, using 5-m PFGI-POFs, we show that extremely high Stokes power can be obtained compared to that of a PFGI-POF with 120- μm core, and estimate the Brillouin threshold power to be 53.3 W. Then, we experimentally show that using a PFGI-POF longer than ~ 50 m is not an effective way to enhance the Stokes signal. We also theoretically predict that it is difficult to decrease the Brillouin threshold power of PFGI-POFs at 1.55- μm wavelength down to that of km-order-long silica SMFs even when their core diameter is sufficiently reduced to satisfy the single-mode condition. Finally, we investigate the Brillouin linewidth as a function of pump power, and confirm the linewidth narrowing effect.

5.1. Motivation

As described in Section 3, the power of the SpBS Stokes light generated in the PFGI-POFs with 120- μm core diameter was quite low, and it needs to be enhanced for detailed investigations of the BGS [39] including the linewidth narrowing effect. Since the BGS observed with the pump-probe technique described in Section 4 is easily influenced by the time constant of lock-in detection, detailed evaluation of its linewidth was not feasible. Another approach to enhance the Stokes signal is to make use of PFGI-POFs with core diameters smaller than 120 μm . Although PFGI-POFs with 62.5- μm core diameter have become commercially available very recently (Sekisui Chemical Co., Ltd., 2011), no study has been reported on their Brillouin scattering properties. Therefore, in this Section, we characterize the BGS in PFGI-POFs with 62.5- μm core diameter.

5.2. Experimental Setup

Irrespective of the length and the core diameter, PFGI-POFs used in the experiment had NA of 0.185, a core refractive index of ~ 1.35 , and propagation loss of ~ 250 dB/km at 1.55 μm . The experimental setup was basically the same as that previously reported in [27], where the BGS can be observed with high resolution by heterodyne detection. A distributed-feedback laser diode (DFB-LD) at 1,547 nm was used as a light source. One end of the PFGI-POF to be measured was optically butt-coupled to the silica SMF, and the other end was kept open.

5.3. Effects of Small Core Diameters

Figure 6 shows the measured BGS of a 5-m PFGI-POF with 62.5- μm core at pump power P_{in} of 5, 10, 15, and 20 dBm. The polarization state optimized for P_{in} of 20 dBm was employed for all the measurements. The center frequency of the BGS, *i.e.*, the BFS, was approximately 2.81 GHz, which is slightly lower than previously-reported value of 2.83 GHz [27] due to the difference in room temperature [30]. Even when P_{in} was as low as 5 dBm, small but clear BGS was observed.

Figure 6. BGS dependence on pump power P_{in} .

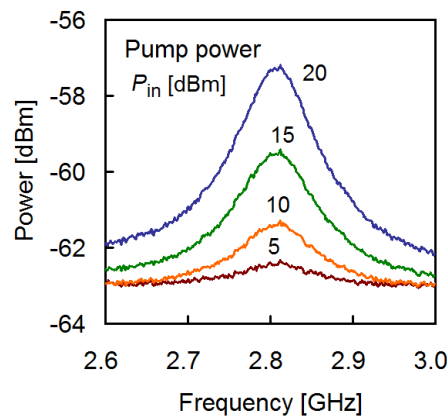
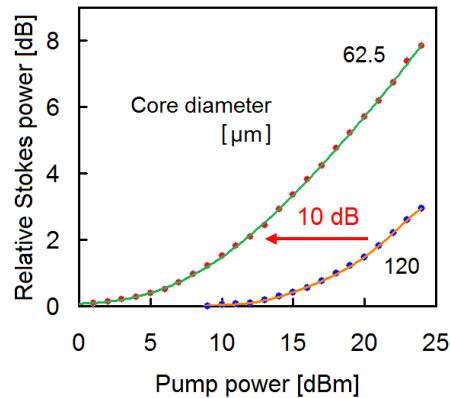


Figure 7 shows the P_{in} dependences of the relative Stokes power, when 5-m PFGI-POFs with core diameters of 62.5 μm and 120 μm (Asahi Glass Co., Ltd., 2009) were employed. The reference power was set to about -63 dBm, which is the Stokes power when P_{in} is sufficiently low. The dependence

curve of the PFGI-POF with 62.5- μm core was about 10 dB lower in pump power than that with 120- μm core, which indicates that, even at the same pump power, we can largely enhance the Stokes signal by using a PFGI-POF with a smaller core diameter.

Figure 7. Relative Stokes power as a function of pump power; comparison between PFGI-POFs with 62.5- μm and 120- μm core diameters.



One of the reasons for the 10-dB curve shift is the difference in Brillouin threshold power P_{th} . By substituting into Equations (1) and (2) the values of $b = 2$ [33], $K = 0.667$ [7], $g_{\text{B}} = 3.09 \times 10^{-11}$ m/W [27], $\alpha = 0.056$ /m (= 250 dB/km), and $L = 5$ m, P_{th} of the PFGI-POF with 120- μm core ($A_{\text{eff}} = 209 \mu\text{m}^2$ [40]) was calculated to be 97.7 W. On the other hand, P_{th} of the PFGI-POF with 62.5- μm core ($A_{\text{eff}} = 108.9 \mu\text{m}^2$) was calculated to be 53.3 W, which is lower than 97.7 W by 2.63 dB. Thus, the curve shift observed in Figure 7 can be partially explained by the difference in P_{th} , but its amount of 10 dB is much larger than the calculated value.

Another reason for the curve shift is the improvement of optical coupling efficiency at the butt coupling when the Stokes light generated in the PFGI-POF propagates back and is injected into the SMF. Although, due to the unstable core alignment and the rough surface of the PFGI-POF, it is difficult to measure the coupling loss accurately, we confirmed that the loss with the PFGI-POF with 62.5- μm core was several dB lower than that with 120- μm core. This fact, along with the difference in internal structure designed by different manufacturers, moderately explains the 10-dB curve shift.

5.4. Effects of Long Fiber Length

According to Equations (1) and (2), to employ long PFGI-POFs is another way to reduce P_{th} and to enhance the Stokes signal. Figure 8 shows the measured BGS of 80-m and 200-m PFGI-POFs with 62.5- μm core at P_{in} of 5, 10, 15, and 20 dBm. Much larger Stokes signals (~ 7 dB higher at P_{in} of 20 dBm) than those of the 5-m PFGI-POF shown in Figure 6 were observed.

There was, however, almost no difference between the BGS of the 80-m PFGI-POF and that of the 200-m PFGI-POF, only with a slight discrepancy of the BFS caused by the room-temperature difference. This means that the incident light is considerably attenuated after propagation for 80 m in the PFGI-POF. In order to estimate this effect quantitatively, the effective PFGI-POF length L_{eff} was plotted as a function of actual length L as shown in Figure 9, where L_{eff} gradually approaches 18 m

($P_{th} \sim 13$ W) with the increasing L . Thus, we proved that employing a PFGI-POF longer than ~ 50 m is not an effective way to enhance the Stokes signal at $1.55 \mu\text{m}$.

Figure 8. BGS dependence on pump power P_{in} ; comparison between 80-m PFGI-POF (solid line) and 200-m PFGI-POF (dotted line).

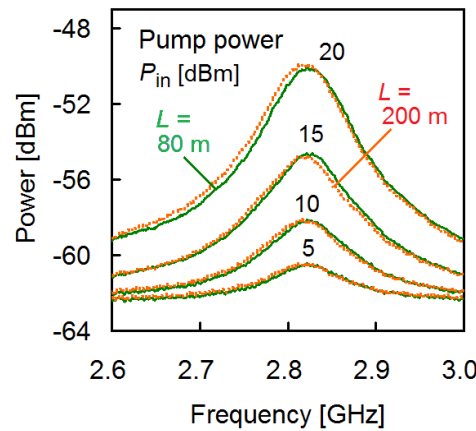
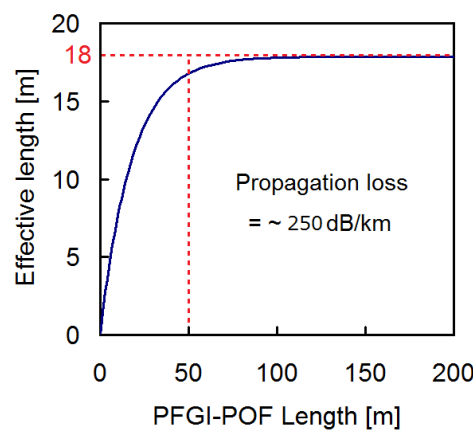


Figure 9. Calculated effective fiber length vs. fiber length.



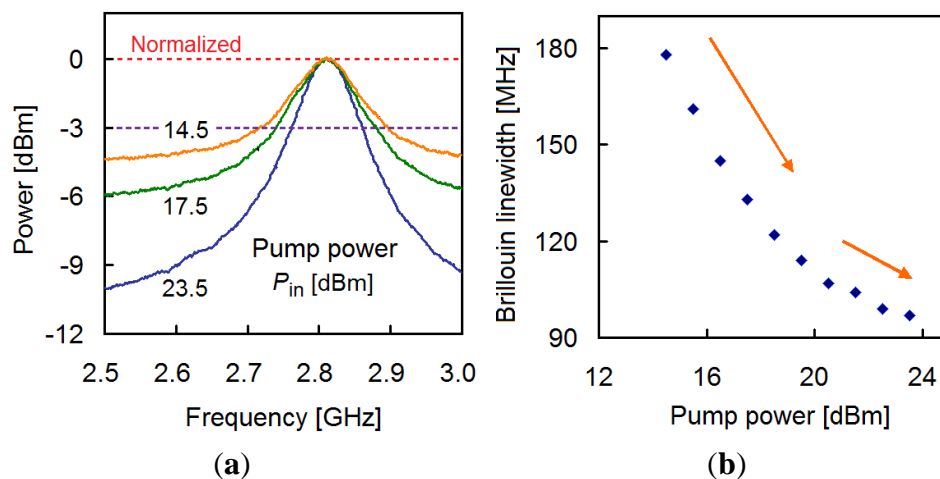
According to Equations (1) and (2), as the core diameter decreases, the Brillouin threshold P_{th} also becomes lower. When P_{in} is higher than P_{th} , SBS is induced and consequently the Stokes signal is exponentially enhanced [7]. Here, under the rough assumption that the multimode nature, NA, refractive index, and loss do not change with core diameters, we calculated P_{th} of a 50-m PFGI-POF with $10\text{-}\mu\text{m}$ core diameter (hypothetical; $A_{eff} = 17.4 \mu\text{m}^2$) to be 2.22 W ($= 33.5$ dBm). This value is more than one order magnitude higher than the pump power of several tens to hundreds of mW commonly used in BGS characterization in silica SMFs [39]. Even when the PFGI-POF is treated as an SMF (*i.e.*, $b = 1$ [7] but A_{eff} becomes larger [35] in Equation (1)), this difference cannot be compensated. Thus, it seems to be difficult to reduce P_{th} of PFGI-POFs down to the same level of that of long silica SMFs by decreasing the core diameter, which is due to the limited effective length of 18 m associated with the high propagation loss at $1.55 \mu\text{m}$.

5.5. Brillouin Linewidth Narrowing Effect

Although the Brillouin linewidth of a PFGI-POF has been reported to be 105 MHz at P_{in} of 20 dBm in [27], detailed investigations were difficult because the Stokes power was extremely low. Here, by making use of the enhanced Stokes power, we investigated the Brillouin linewidth dependence on P_{in} .

Figure 10(a) shows the measured BGS of the 200-m PFGI-POF with 62.5- μm core at P_{in} of 14.5, 17.5, and 23.5 dBm, where the Stokes power is normalized so that the maximum power is 0 dB. Figure 10(b) shows the Brillouin linewidth dependence on P_{in} . From these figures, we can see that, with the increasing P_{in} , the 3-dB linewidth of the BGS decreases, but that its slope gradually becomes small. This behavior agrees well with the experiment and theory of the linewidth narrowing effect in silica-based SMFs [39].

Figure 10. (a) Normalized BGS at pump power of 14.5, 17.5, and 23.5 dBm. (b) Brillouin linewidth vs. pump power.



5.6. Summary

The BGS properties of PFGI-POFs with 62.5- μm core diameter were investigated. The Stokes power was extremely high compared to that of a PFGI-POF with 120- μm core, and the Brillouin threshold power for 5-m PFGI-POF was estimated to be 53.3 W. It was also shown that employing a PFGI-POF longer than ~ 50 m is not an effective way to enhance the Stokes signal. In addition, it was theoretically found that it is difficult to reduce the Brillouin threshold power of PFGI-POFs at 1.55- μm wavelength below that of long silica SMFs even if their core diameter is sufficiently decreased to satisfy the single-mode condition. Finally, the Brillouin linewidth narrowing effect was confirmed. These results will be a good guideline for developing practical Brillouin systems using PFGI-POFs as well as for designing new PFGI-POF structures for Brillouin applications in future.

6. Conclusions

We reviewed two methods of enhancing the Brillouin Stokes signal in PFGI-POFs for future practical applications as well as for detailed investigations of the BGS.

In the first half of this paper, using an experimental setup similar to BOCDA system [16,17] based on the pump-probe technique, SBS in a PFGI-POF with 120- μm core diameter was, for the first time, observed at 1.55 μm . The BGS was detected with extremely high S/N ratio, even with a 1-m PFGI-POF, scrambled polarization state, and no averaging. We also investigated the BGS dependences on probe power and temperature, and confirmed that SBS in a PFGI-POF measured with this technique can also be utilized to develop high-accuracy temperature sensors.

In the latter half, the influence of the core diameter and fiber length on the Stokes signal was investigated by use of PFGI-POFs with 62.5- μm core diameter. First, using 5-m PFGI-POFs, we showed that extremely high Stokes power can be obtained compared to that of a PFGI-POF with 120- μm core, and estimated the Brillouin threshold power to be 53.3 W. Then, we experimentally showed that using a PFGI-POF longer than ~ 50 m is not an effective way to enhance the Stokes signal. We also theoretically predicted that it is difficult to decrease the Brillouin threshold power of PFGI-POFs at 1.55- μm wavelength down to that of km-order-long silica SMFs even when their core diameter is sufficiently reduced to satisfy the single-mode condition. Finally, we investigated the Brillouin linewidth as a function of pump power, and confirmed the linewidth narrowing effect.

Thus, the Brillouin Stokes signal has been drastically enhanced. It is also natural to predict that the Stokes signal will be further enhanced if we induce SBS by pump-probe technique using PFGI-POFs with 62.5- μm core diameter or less. Therefore, we are sure that the first demonstration of distributed temperature sensing based on Brillouin scattering in PFGI-POFs will be possibly carried out in the near future, based on optical correlation-, time-, or frequency-domain technology. We believe our work to be a significant technological step toward the implementation of such sensing systems and other POF-Brillouin devices.

Acknowledgements

We are indebted to Kazuo Hotate and Masato Kishi of the University of Tokyo, Japan, for allowing us to use their experimental facilities. We also acknowledge Takaaki Ishigure of Keio University, Japan, for his helpful comments and discussions. Y. Mizuno is grateful to the Research Fellowships for Young Scientists from the Japan Society for the Promotion of Science (JSPS).

References

1. Kuzyk, M.G. *Polymer Fiber Optics: Materials, Physics, and Applications*, 1st ed.; CRC Press: Boca Raton, FL, USA, 2006.
2. Koike, Y.; Ishigure, T.; Nihei, E. High-bandwidth graded-index polymer optical fiber. *J. Lightwave Technol.* **1995**, *13*, 1475-1489.
3. Husdi, I.R.; Nakamura, K.; Ueha, S. Sensing characteristics of plastic optical fibres measured by optical time-domain reflectometry. *Meas. Sci. Technol.* **2004**, *15*, 1553-1559.
4. Mollers, I.; Jager, D.; Gaudino, R.; Nocivelli, A.; Kragl, H.; Ziemann, O.; Weber, N.; Koonen, T.; Lezzi, C.; Bluschke, A.; *et al.* Plastic optical fiber technology for reliable home networking—Overview and results of the EU project POF-ALL. *IEEE Commun. Mag.* **2009**, *47*, 58-68.

5. Liehr, S.; Lenke, P.; Wendt, M.; Krebber, K.; Seeger, M.; Thiele, E.; Metschies, H.; Gebreselassie, B.; Munich, J.C. Polymer optical fiber sensors for distributed strain measurement and application in structural health monitoring. *IEEE Sens. J.* **2009**, *9*, 1330-1338.
6. Ippen, E.P.; Stolen, R.H. Stimulated Brillouin scattering in optical fibers. *Appl. Phys. Lett.* **1972**, *21*, 539-541.
7. Agrawal, G.P. *Nonlinear Fiber Optics*, 4th ed.; Academic Press: San Diego, CA, USA, 1995; pp. 329-367.
8. Cowle, G.J.; Yu, D.; Chieng, Y.T. Brillouin/erbium fiber lasers. *J. Lightwave Technol.* **1997**, *15*, 1198-1204.
9. Norcia, S.; Tonda-Goldstein, S.; Dolfi, D.; Huignard, J.P. Efficient single-mode Brillouin fiber laser for low-noise optical carrier reduction of microwave signals. *Opt. Lett.* **2003**, *28*, 1888-1890.
10. Song, K.Y.; Herraiez, M.G.; Thevenaz, L. Observation of pulse delaying and advancement in optical fibers using stimulated Brillouin scattering. *Opt. Express* **2005**, *13*, 82-88.
11. Kuzin, E.A.; Petrov, M.P.; Davydenko, B.E. Phase conjugation in an optical fibre. *Opt. Quantum Electron.* **1985**, *17*, 393-397.
12. Zou, W.; He, Z.; Hotate, K. Tunable fiber-optic delay line based on stimulated Brillouin scattering. *Appl. Phys. Express* **2010**, *3*, doi:10.1143/APEX.3.012501.
13. Zhu, Z.; Gauthier, D.J.; Boyd, R.W. Stored light in an optical fiber via stimulated Brillouin scattering. *Science* **2007**, *318*, 1748-1750.
14. Mizuno, Y.; Nakamura, K. Core alignment of butt-coupling between single-mode and multi-mode optical fibers by monitoring Brillouin scattering signal. *J. Lightwave Technol.* **2011**, *29*, 2616-2620.
15. Horiguchi, T.; Tateda, M. BOTDA—Nondestructive measurement of single-mode optical fiber attenuation characteristics using Brillouin interaction: Theory. *J. Lightwave Technol.* **1989**, *7*, 1170-1176.
16. Hotate, K.; Hasegawa, T. Measurement of Brillouin gain spectrum distribution along an optical fiber using a correlation-based technique—Proposal, experiment and simulation. *IEICE Trans. Electron.* **2000**, *E83-C*, 405-412.
17. Song, K.Y.; Hotate, K. Enlargement of measurement range in a Brillouin optical correlation domain analysis system using double lock-in amplifiers and a single-sideband modulator. *IEEE Photon. Technol. Lett.* **2006**, *18*, 499-501.
18. Mizuno, Y.; Zou, W.; He, Z.; Hotate, K. Proposal of Brillouin optical correlation-domain reflectometry (BOCDR). *Opt. Express* **2008**, *16*, 12148-12153.
19. Abedin, K.S. Stimulated Brillouin scattering in single-mode tellurite glass fiber. *Opt. Express* **2006**, *14*, 11766-11772.
20. Mizuno, Y.; He, Z.; Hotate, K. Distributed strain measurement using a tellurite glass fiber with Brillouin optical correlation-domain reflectometry. *Opt. Commun.* **2010**, *283*, 2438-2441.
21. Abedin, K.S. Observation of strong stimulated Brillouin scattering in single-mode As₂Se₃ chalcogenide fiber. *Opt. Express* **2005**, *13*, 10266-10271.
22. Song, K.Y.; Abedin, K.S.; Hotate, K.; Herraiez, M.G.; Thevenaz, L. Highly efficient Brillouin slow and fast light using As₂Se₃ chalcogenide fiber. *Opt. Express* **2006**, *14*, 5860-5865.

23. Lee, J.H.; Tanemura, T.; Kikuchi, K.; Nagashima, T.; Hasegawa, T.; Ohara, S.; Sugimoto, N. Experimental comparison of a Kerr nonlinearity figure of merit including the stimulated Brillouin scattering threshold for state-of-the-art nonlinear optical fibers. *Opt. Lett.* **2005**, *30*, 1698-1700.
24. Mizuno, Y.; He, Z.; Hotate, K. Dependence of the Brillouin frequency shift on temperature in a tellurite glass fiber and a bismuth-oxide highly-nonlinear fiber. *Appl. Phys. Express* **2009**, *2*, 112402:1-112402:3.
25. Lee, J.H.; Yusoff, Z.; Belardi, W.; Ibsen, M.; Monro, T.M.; Richardson, D.J. Investigation of Brillouin effects in small-core holey optical fiber: Lasing and scattering. *Opt. Lett.* **2002**, *27*, 927-929.
26. Beugnot, J.C.; Sylvestre, T.; Alasia, D.; Maillotte, H.; Laude, V.; Monteville, A.; Provino, L.; Traynor, N.; Mafang, S.F.; Thevenaz, L. Complete experimental characterization of stimulated Brillouin scattering in photonic crystal fiber. *Opt. Express* **2007**, *15*, 15517-15522.
27. Mizuno, Y.; Nakamura, K. Experimental study of Brillouin scattering in perfluorinated polymer optical fiber at telecommunication wavelength. *Appl. Phys. Lett.* **2010**, *97*, doi:10.1063/1.3463038.
28. Mizuno, Y.; Nakamura, K. Brillouin scattering in polymer optical fibers: Fundamental properties and potential use in sensors. *Polymers* **2011**, *3*, 886-898.
29. Lethien, C.; Loyez, C.; Vilcot, J.-P.; Rolland, N.; Rolland, P.A. Exploit the bandwidth capacities of the perfluorinated graded index polymer optical fiber for multi-services distribution. *Polymers* **2011**, *3*, 1006-1028.
30. Mizuno, Y.; Nakamura, K. Potential of Brillouin scattering in polymer optical fiber for strain-insensitive high-accuracy temperature sensing. *Opt. Lett.* **2010**, *35*, 3985-3987.
31. Mizuno, Y.; Kishi, M.; Hotate, K.; Ishigure, T.; Nakamura, K. Observation of stimulated Brillouin scattering in polymer optical fiber with pump-probe technique. *Opt. Lett.* **2011**, *36*, 2378-2380.
32. Mizuno, Y.; Ishigure, T.; Nakamura, K. Brillouin gain spectrum characterization in perfluorinated graded-index polymer optical fiber with 62.5- μm core diameter. *IEEE Photon. Technol. Lett.* **2011**, *23*, 1863-1865.
33. Tei, K.; Tsuruoka, Y.; Uchiyama, T.; Fujioka, T. Critical power of stimulated Brillouin scattering in multimode optical fibers. *Jpn. J. Appl. Phys.* **2001**, *40*, 3191-3194.
34. Marcuse, D. Loss analysis of single-mode fiber splices. *Bell Sys. Tech. J.* **1977**, *56*, 703-718.
35. Mocofanescu, A.; Wang, L.; Jain, R.; Shaw, K.D.; Gavrielides, A.; Peterson, P.; Sharma, M.P. SBS threshold for single mode and multimode GRIN fibers in an all fiber configuration. *Opt. Express* **2005**, *13*, 2019-2024.
36. Horiguchi, T.; Kurashima, T.; Tateda, M. Tensile strain dependence of Brillouin frequency shift in silica optical fibers. *IEEE Photon. Technol. Lett.* **1989**, *1*, 107-109.
37. Kurashima, T.; Horiguchi, T.; Tateda, M. Thermal effects on the Brillouin frequency shift in jacketed optical silica fibers. *Appl. Opt.* **1990**, *29*, 2219-2222.
38. Shibata, N.; Azuma, Y.; Horiguchi, T.; Tateda, M. Identification of longitudinal acoustic mode guided in the core region of a single-mode optical fiber by Brillouin gain spectra measurements. *Opt. Lett.* **1988**, *13*, 595-597.
39. Yeniay, A.; Delavaux, J.M.; Toulouse, J. Spontaneous and stimulated Brillouin scattering gain spectra in optical fibers. *J. Lightwave Technol.* **2002**, *20*, 1425-1432.

40. Dossou, M.; Szriftgiser, P.; Goffin, A. Theoretical study of stimulated Brillouin scattering (SBS) in polymer optical fibres. In *13th Annual Symposium IEEE/LEOS Benelux Chapter*, Enschede, The Netherlands, 2008; volume 13, 175-178.

© 2012 by the authors; licensee MDPI, Basel, Switzerland. This article is an open access article distributed under the terms and conditions of the Creative Commons Attribution license (<http://creativecommons.org/licenses/by/3.0/>).